IEEE Access
Multidisciplinary | Rapid Review | Open Access Journal

Received August 11, 2019, accepted August 29, 2019, date of publication September 2, 2019,
date of current version September 19, 2019.

Digital Object Identifier 10.1109/ACCESS.2019.2939085

Harmonic Analysis in Gaseous Helium by Coherent Schrödinger-Maxwell Method

LEI ZHANG, ZHENHONG FAN, AND RUSHAN CHEN, (Senior Member, IEEE)
Department of Communication Engineering, Nanjing University of Science and Technology, Nanjing 210094, China

Corresponding author: Zhenhong Fan (zhfan@njust.edu.cn)

This work was supported in part by the National Natural Science Foundation of China under Grant 61431006 and Grant 61871443.

ABSTRACT This paper concentrates on harmonic analysis in gaseous helium, including microscopic generation, selective filtration and macroscopic propagation. A coherent method is proposed, with time-dependent Schrödinger equation for harmonic generation and Maxwell's wave equation for harmonic propagation. By introducing the polarization source based on the microscopic single-atom response, the macroscopic nonlinear propagation can be efficiently solved by a set of linear equations at each harmonic frequency. Using the proposed method, we numerically investigate the propagation effects of selective harmonics in gaseous helium. Our results reveal that specific harmonics allow the synthesis of an isolated attosecond pulse, which presents a high beam quality and an excellent spatial profile with Gaussian-like distribution. Moreover, the generated pulse provides a promising potential on high power defense, quantum radar and communication.

INDEX TERMS Gaseous helium, harmonic analysis, Maxwell's wave equation, propagation effects, time-dependent Schrödinger equation.

I. INTRODUCTION

Harmonic analysis is a mathematic branch associated with the basic signal or wave, which has become a vast subject with applications on communication, signal processing and quantum mechanics [1]. Generally, low-order harmonics may occur in electronic devices at microwave range [2], plasmonic structures at terahertz range [3] and metal nanoparticles at visible-light [4]. With the development of high intensity lasers, harmonics of tens- and hundreds-order are observed from gaseous medium by intense driving field [5]. High-order harmonic generation (HHG) has attracted considerable attentions due to its practical application to synthesize isolated attosecond (as, 10^{-18}s) pulse (IAP) [6]. The IAP presents extremely close to the ideal impulse with wide frequency band, which makes it a promising candidate on input pulse for high power defense [7] and transmitting signal for quantum radar and communication [8], [9].

As shown in Fig. 1, typical high-order harmonic spectra begin with a rapid decline for low-order harmonics consistent with the perturbation theory [10], followed by a broad plateau of almost constant intensity, and vanish with an abrupt cutoff. A breakthrough understanding with a "three-step model" [11] was initiated by Corkum to explain the plateau effect in HHG spectra, which involved ionization away from the nucleus, propagation in the driving field, and recombination with the parent ion. To quantitatively calculate harmonics at each order, classical theory [12], semiclassical theory [13], and theory of quantum electrodynamics [14], [15] are widely used to describe the microscopic interaction between an atom and an intense driving field.

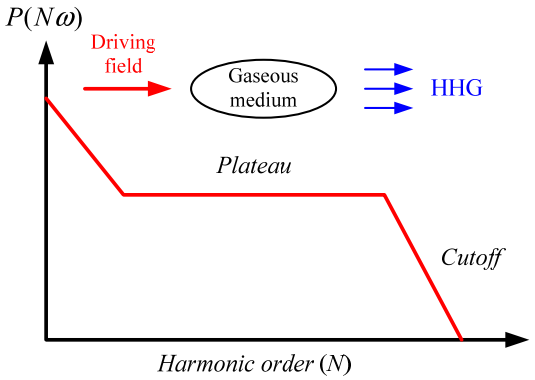

FIGURE 1. Typical high-order harmonic spectra from gaseous medium, which begin with a rapid decline on intensity for low-order harmonics, followed by a broad plateau of almost constant intensity, and vanish with an abrupt cutoff.

The associate editor coordinating the review of this article and approving it for publication was Firuz Zare.

However, a complete description of high-order harmonic analysis consists of three parts: microscopic harmonic generation by the intense driving field, selective filtration for IAP synthetization and macroscopic propagation of relevant harmonic fields in gaseous medium [16]. According to the relationship between time domain and frequency domain, broad frequency band corresponds narrow time band. Therefore, harmonics in the plateau region are made full use for IAP synthetization. As is well known, Fourier transform [17] is a mathematical tool used in signal processing and analysis. Unfortunately, it can not reflect the local correspondence between short time and frequency. Using a ''reverse, shift, multiply and integrate'' technique, wavelet transform can overcome this disadvantage to analyze local time-frequency relationship of non-stationary signal [18]. Thus, in the process of selective filtration, wavelet transform is usually utilized to investigate the time-frequency characteristic of high-order harmonics in the plateau region.

In the previous work [16], attosecond pulses have been synthetized by harmonics of microscopic single-atom response. Furthermore, macroscopic propagation of relevant harmonic fields in gaseous medium should be considered for spatial distribution of the generated IAP. Frequency domain methods can be used to model nonlinear harmonic phenomena to avoid cumbersome media dispersion in time domain. For low-order harmonics, Xiong *et al.* [19] proposed a surface integral equation (SIE) method to solve the coupled-wave equations for second- harmonic generation and radiation. Fang *et al.* [20] established a full hydrodynamic model to simulate nonlinear harmonic response and distribution in metallic metamaterials. For high-order harmonics, Jin *et al.* [21] investigated medium propagation effects in Ar and N_2, with an approximate nonlinear polarization source based on quantitative rescattering (QRS) theory [22]. Besides, many efforts have been made on IAP propagation effects of beam quality and spatial profile due to its crucial role for experimental measurement [23], [24].

In this paper, a coherent method is proposed for harmonic analysis in gaseous helium, including microscopic generation, selective filtration and macroscopic propagation. First, we solve the time-dependent Schrödinger equation (TDSE) [25] to obtain accurate harmonic spectra. Then Morlet wavelet transform [18] is applied to investigate the time-frequency characteristic of harmonics for selective filtration. Finally, the generated IAP with broad band is investigated by Maxwell's wave equations at each harmonic frequency, with nonlinear polarization source based on the microscopic single-atom response. The main contribution is that the nonlinear harmonic propagation can be accurately solved at certain harmonic frequency with a set of linear equations. In order to improve efficiency and stability, the Crank-Nicholson (CN) difference scheme [26] is employed in whole procedure. Using the proposed method, we numerically investigate the propagation effects of selective harmonics in gaseous helium. The simulated results reveal that specific harmonics are able to synthesize an isolated attosecond pulse which presents a high beam quality and an excellent spatial profile with Gaussian-like distribution. Moreover, the generated pulse provides a promising potential on high power defense, quantum radar and communication.

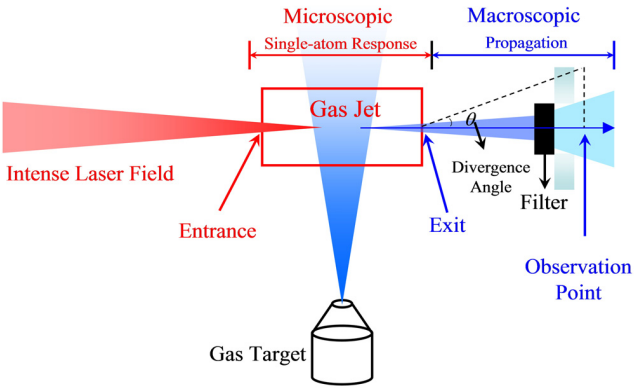

FIGURE 2. Illustration of a complete typical HHG spectra observation.

The paper is organized as follows: Section I is the introduction. Section II gives the formulations of microscopic generation, selective filtration and macroscopic propagation. In section III, some numerical results are presented to demonstrate the accuracy, efficiency and practical value of the proposed method. A brief conclusion is given in section IV.

II. PRINCIPLE AND FORMULATION

As shown in Fig. 2, a complete description of high-order harmonic spectra observed experimentally consists of three parts: microscopic harmonic generation, selective filtration and macroscopic propagation. First, harmonics may occur in the gas jet due to single-atom response between gaseous target and driving intense laser field. Then, a filter is located near the exit of gas jet for selective filtration to synthetize IAP. During the propagation, the peak center of IAP with relevant harmonic fields will diverge, resulting in a divergence angle.

A. MICROSCOPIC HIGH-ORDER HARMONIC GENERATION

According to the mentioned ''three-step model'' [11], an outmost electron is driven away from the nucleus by the intense laser field. When the oscillating laser field changes its sign, the electron decelerates to zero and re-accelerate back towards the parent ion. If the returning electron recombines with its parent ion, high-order harmonics can be released with high energy photon, which is much larger than that of the fundamental field. The entire interaction between gaseous atom and intense laser field can be solved by TDSE expressed as:

$$i\hbar\frac{\partial}{\partial t}\psi(\vec{r},t)=\left[-\frac{\hbar^2}{2m_e}\nabla^2+V(\vec{r})-e\vec{r}\cdot\vec{E}(t)\right]\psi(\vec{r},t) \tag{1}$$

where $i=\sqrt{-1}$, $\psi(\vec{r},t)$ is the wave function, $\hbar$ is reduced Planck's constant, m_e is the real mass of the valence electron,

$\nabla^2 = \partial^2/\partial r^2$, $V(\vec{r})$ is the potential energy distribution of gaseous atom, and $\vec{E}(t)$ is the driving intense laser field.

Using Crank-Nicholson difference scheme, equation (1) is solved by the finite difference time domain (FDTD) method with 3-D stability condition [16]:

$$2\Delta t\left[\frac{1}{(\Delta x)^2}+\frac{1}{(\Delta y)^2}+\frac{1}{(\Delta z)^2}\right]+\Phi_{\max}\Delta t \le 2 \quad (2)$$

where $\Phi(\vec{r},t) = V(\vec{r}) - e\vec{r}\cdot\vec{E}(t)$.

According to Ehrenfest theorem [27], the electron average acceleration $a(t)$ can be calculated by mathematical expectation expressed as:

$$\begin{aligned} a(t) &= \left\langle \psi(\vec{r},t)\left|-\frac{\partial\Phi(\vec{r},t)}{\partial r}\right|\psi(\vec{r},t)\right\rangle \\ &= \int_\Omega \psi^*(\vec{r},t)\left[-\frac{\partial\Phi(\vec{r},t)}{\partial r}\right]\psi(\vec{r},t)d\Omega \end{aligned} \quad (3)$$

where Ω is the total computational space.

Generally, the intensity of high-order harmonic at each order is expressed as:

$$P(\omega) \propto |a(\omega)|^2 = \left|\int_0^t a(t)e^{-i\omega t}dt\right|^2 \quad (4)$$

B. SELECTIVE FILTRATION

According to the relationship between time domain and frequency domain, broad frequency band corresponds narrow time band. To make full use of harmonic orders in the plateau region, we apply Morlet wavelet transform into the analysis of non-stationary signal by high-order harmonic generation. By adding a window function with adjustable width, Morlet wavelet transform automatically narrows the width of the time window as the signal frequency increases, greatly improving the resolution. The expression of Morlet wavelet transform is as follows:

$$\begin{aligned} A_\omega(t_c,\omega) &= \int_{-\infty}^{+\infty} h(t)w_{t_c,\omega}(t)dt \\ &= \int_{-\infty}^{+\infty} \sqrt{\omega}h(t)W\left[\omega\left(t-t_c\right)\right]dt \end{aligned} \quad (5)$$

where $w_{t_c,\omega}(t)$ indicates the kernel function with $W(x)$ defined as:

$$W(x) = \left(\frac{1}{\sqrt{\tau}}\right)\exp(ix)\exp\left(-\frac{x^2}{2\tau^2}\right) \quad (6)$$

in which τ is the window width of Morlet wavelet transform.

After wavelet transform applied, the correspondence of harmonics intensity in different time and frequency can obtained. Therefore, an IAP may be achieved by

$$I(t) = \left|\sum_{m=N_1}^{N_2} a(\omega)e^{im\omega t}\right|^2 \quad (7)$$

with $[N_1, N_2]$ is the suitable order range from plateau region in Fig. 1.

C. MACROSCOPIC HARMONIC PROPAGATION

In HHG experiments, the IAP with broad frequency band carries out a macroscopic propagation in gaseous medium until observation. During propagation, the intensity and distribution of harmonics will change due to the interaction of gaseous medium, resulting in a divergence angle compared with ideal impulse, which can not be ignored. In our work, by introducing nonlinear polarization source based on microscopic single-atom response, propagation of the generated IAP with broad band in gaseous medium is investigated by Maxwell's wave equations at each harmonic frequency. The CN difference scheme is employed in the entire solution, to improve efficiency and stability.

1) MAXWELL'S WAVE EQUATION

With the symmetry of spatial distribution in cylindrical coordinate system, Maxwell's wave equation for the propagation of high-order harmonics is expressed as:

$$\nabla^2 E_h(r,z,t) - \frac{1}{c^2}\frac{\partial^2}{\partial t^2}E_h(r,z,t) = \frac{1}{\varepsilon_0 c^2}\frac{\partial^2}{\partial t^2}P_{NL}(r,z,t) \quad (8)$$

where $\nabla^2 = \nabla_\perp^2 + \partial^2/\partial z^2$ indicates the Laplace operator in cylindrical coordinate system, $E_h(r,z,t)$ is the high-order harmonic field, $P_{NL}(r,z,t)$ is the nonlinear polarization source depended upon the applied fundamental field $E_1(r,z,t)$, c is the velocity of light in vacuum and ε_0 is the permittivity of vacuum.

For the sake of calculation, we employ motion coordinate system with $z' = z$ and $t' = t - z/c$, then the time and space partial derivatives are defined as:

$$\begin{cases} \dfrac{\partial}{\partial z} = \dfrac{\partial}{\partial z'} - \dfrac{1}{c}\dfrac{\partial}{\partial t'}, & (a) \\ \dfrac{\partial}{\partial t} = \dfrac{\partial}{\partial t'}, & (b) \\ \dfrac{\partial^2}{\partial z^2} = \dfrac{\partial^2}{\partial z'^2} - \dfrac{2}{c}\dfrac{\partial^2}{\partial z'\partial t'} + \dfrac{1}{c^2}\dfrac{\partial^2}{\partial t'^2}, & (c) \\ \dfrac{\partial^2}{\partial t^2} = \dfrac{\partial^2}{\partial t'^2}, & (d) \end{cases} \quad (9)$$

Under the slowly evolving wave approximation [28], the order of $\partial^2/\partial z'^2$ is much less than that of $\partial/\partial z'$, so the first item in Eq. (9.c) on the right hand can be ignored. Substituting Eq. (9) into Eq. (8), we can obtain Maxwell wave equation of macroscopic HHG propagation in motion coordinate system as:

$$\begin{aligned} &\nabla_\perp^2 E_h\left(r,z',t'\right) - \frac{2}{c}\frac{\partial^2}{\partial z'\partial t'}E_h\left(r,z',t'\right) \\ &\qquad = \frac{1}{\varepsilon_0 c^2}\frac{\partial^2}{\partial t'^2}P_{NL}\left(r,z',t'\right) \end{aligned} \quad (10)$$

In order to further simplify calculation, Fourier transform is applied into Eq. (10) to obtain Maxwell wave equation in frequency domain as:

$$\begin{aligned} &\nabla_\perp^2 \tilde{E}_h\left(r,z',\omega_n\right) - \frac{2i\omega_h}{c}\frac{\partial\tilde{E}_h\left(r,z',\omega_h\right)}{\partial z'} \\ &\qquad = -\frac{\omega_h^2}{\varepsilon_0 c^2}\tilde{P}_{NL}\left(r,z',\omega_h\right) \end{aligned} \quad (11)$$

where $\tilde{E}_h\left(r, z', \omega_h\right)$ and $\tilde{P}_{NL}\left(r, z', \omega_h\right)$ are the component of high-order harmonics and nonlinear polarization source at h-th order frequency ω_h, respectively. Once the nonlinear polarization source $\tilde{P}_{NL}\left(r, z', \omega_h\right)$ is given, the spatial distribution of macroscopic propagation effects can be achieved by Eq. (11) with CN difference method.

2) CRANK-NICHOLSON DIFFERENCE METHOD

The Laplace operator in cylindrical coordinate system is expressed as:

$$\nabla_{\perp}^2 f = \frac{\partial^2 f}{\partial r^2} + \frac{1}{r}\frac{\partial f}{\partial r} + \frac{\partial^2 f}{\partial \varphi^2}\frac{1}{r} \tag{12}$$

Substituting Eq. (12) into Eq. (11), we can obtain:

$$\frac{2i\omega_h}{c}\frac{\partial \tilde{E}_h\left(r, z', \omega_h\right)}{\partial z'} = \frac{\partial^2 \tilde{E}_h\left(r, z', \omega_h\right)}{\partial r^2} + \frac{1}{r}\frac{\partial \tilde{E}_h\left(r, z', \omega_h\right)}{\partial r} + \frac{\omega_h^2}{\varepsilon_0 c^2}\tilde{P}_{NL}\left(r, z', \omega_h\right) \tag{13}$$

Then Eq. (13) can be exactly solved by Crank-Nicholson difference method as Eqs. (14.a) and (14.b) shown at the bottom of the current page. It should be mentioned that L'hôpital's Rule [29] is employed for Eq. (14.b) to eliminate singular item $1/r$ in Eq. (14.a) with:

$$\lim_{r\to 0}\left(\frac{1}{r}\frac{\partial E}{\partial r}\right) = \lim_{r\to 0}\left(\frac{1}{r'}\left(\frac{\partial E}{\partial r}\right)'\right) = \left.\frac{\partial^2 E}{\partial r^2}\right|_{r\to 0} \tag{15}$$

As a consequence, problem (14) can be solved by tridiagonal matrix algorithm [30] without direct inverse.

3) NONLINEAR POLARIZATION SOURCE

The component of nonlinear polarization source at each harmonic frequency is decided by the Fourier transform of nonlinear polarization response, as:

$$P_{NL}\left(r, z', t\right) = \left[n_0 - n_e\left(r, z', t\right)\right]\langle x\left(t\right)\rangle \tag{16}$$

where n_0 is the initial neutral atom density in gas medium, $\langle x\left(t\right)\rangle$ is the time dependent dipole moment in microscopic single-atom response defined as:

$$\langle x\left(t\right)\rangle = \langle \varphi\left(r, t\right)|r|\,\varphi\left(r, t\right)\rangle \tag{17}$$

TABLE 1. Conversion between hartree atomic units and international system of units.

Parameter	Hartree atomic units (a.u.)	International system of units (SI)
Plank's constant	2π	$6.626075443\times10^{-34} J\cdot s$
Charge	1	$1.60217733\times10^{-19} C$
Mass	1	$9.1093897\times10^{-31} kg$
Length	1	$5.29177249\times10^{-11} m$
Time	1	$2.41888129\times10^{-17} s$
Frequency	1	$4.13414251\times10^{16} s^{-1}$

and $n_e\left(r, z', t\right)$ is the density of free electron calculated by:

$$n_e\left(r, z', t\right) = n_0\left[1 - \exp\left(-\int_{-\infty}^{t}\gamma\left(r, z', t'\right)dt'\right)\right] \tag{18}$$

where $\gamma\left(r, z', t'\right)$ is the ionization rate calculated from Ammosov-Delone-Krainov (ADK) theory [31].

III. NUMERICAL RESULTS

In this section, we investigated both microscopic single-atom response and macroscopic propagation effects of high-order harmonics fields from helium atom by intense two-color Bessel-Gauss (BG) beam [23], [24]. In atomic physics, Hartree atomic units (a.u.) are widely applied to avoid the conversion between units for computer precision [32], as shown in Table 1. In this case, the helium atom is established by one dimensional soft core Coulomb potential model with [33]

$$V\left(x\right) = -\frac{1}{\sqrt{x^2 + 0.484}} \tag{19}$$

As shown in Fig. 3, the two-color BG beam E_{BG} is synthesized by a fundamental pulse E_0 with linearly polarized (central $\lambda_0 = 800nm$) and a control pulse E_1 with linearly polarized (central $\lambda_1 = 1600nm$), given by:

$$E_{BG}\left(r, z, t\right) = E_0\left(r, z\right)f_0\left(t\right)\cos\left(\omega_0 t\right) + E_1\left(r, z\right)f_1\left(t\right)\cos\left(0.5\omega_0 t + \phi_1\right) \tag{20}$$

$$\begin{aligned}
&-\frac{\Delta z'}{2\left(\Delta r\right)^2}\tilde{E}_h\left(r_{n-1}, z'_{m+1}, \omega_h\right) + \left(\frac{2i\omega_h}{c} + \frac{\Delta z'}{\left(\Delta r\right)^2} + \frac{\Delta z'}{2r\left(\Delta r\right)}\right)\tilde{E}_h\left(r_n, z'_{m+1}, \omega_h\right) - \left(\frac{\Delta z'}{2\left(\Delta r\right)^2} + \frac{\Delta z'}{2r\left(\Delta r\right)}\right)\tilde{E}_h\left(r_{n+1}, z'_{m+1}, \omega_h\right)\\
&= \frac{\Delta z'}{2\left(\Delta r\right)^2}\tilde{E}_h\left(r_{n-1}, z'_m, \omega_h\right) + \left(\frac{2i\omega_h}{c} - \frac{\Delta z'}{\left(\Delta r\right)^2} - \frac{\Delta z'}{2r\left(\Delta r\right)}\right)\tilde{E}_h\left(r_n, z'_m, \omega_h\right)\\
&\quad + \left(\frac{\Delta z'}{2\left(\Delta r\right)^2} + \frac{\Delta z'}{2r\left(\Delta r\right)}\right)\tilde{E}_h\left(r_{n+1}, z'_m, \omega_h\right) + \frac{\omega_h^2}{\varepsilon_0 c^2}\tilde{P}_{NL}\left(r_n, z'_m, \omega_h\right), \quad r \neq 0
\end{aligned} \tag{14.a}$$

$$\begin{aligned}
&-\frac{\Delta z'}{\left(\Delta r\right)^2}\tilde{E}_h\left(r_{n-1}, z'_{m+1}, \omega_h\right) + \left(\frac{2i\omega_h}{c} + \frac{2\Delta z'}{\left(\Delta r\right)^2}\right)\tilde{E}_h\left(r_n, z'_{m+1}, \omega_h\right) - \left(\frac{\Delta z'}{\left(\Delta r\right)^2}\right)\tilde{E}_h\left(r_{n+1}, z'_{m+1}, \omega_h\right)\\
&= \frac{\Delta z'}{\left(\Delta r\right)^2}\tilde{E}_h\left(r_{n-1}, z'_m, \omega_h\right) + \left(\frac{2i\omega_h}{c} - \frac{2\Delta z'}{\left(\Delta r\right)^2}\right)\tilde{E}_h\left(r_n, z'_m, \omega_h\right) + \left(\frac{\Delta z'}{\left(\Delta r\right)^2}\right)\tilde{E}_h\left(r_{n+1}, z'_m, \omega_h\right)\\
&\quad + \frac{\omega_h^2}{\varepsilon_0 c^2}\tilde{P}_{NL}\left(r_n, z'_m, \omega_h\right), \quad r = 0
\end{aligned} \tag{14.b}$$

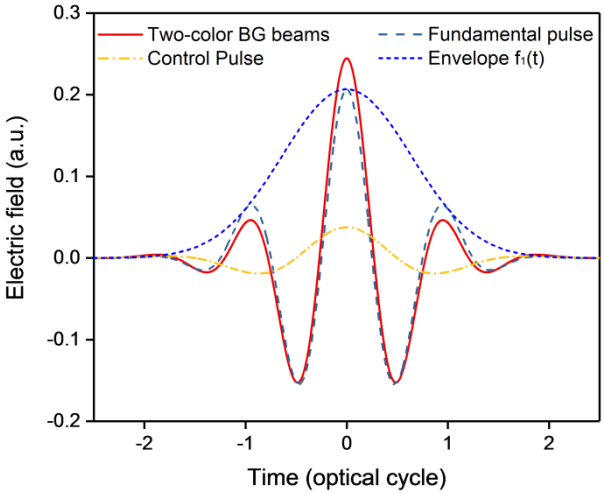

FIGURE 3. The intense two-color bessel-gauss beam synthesized by fundamental and control pulse.

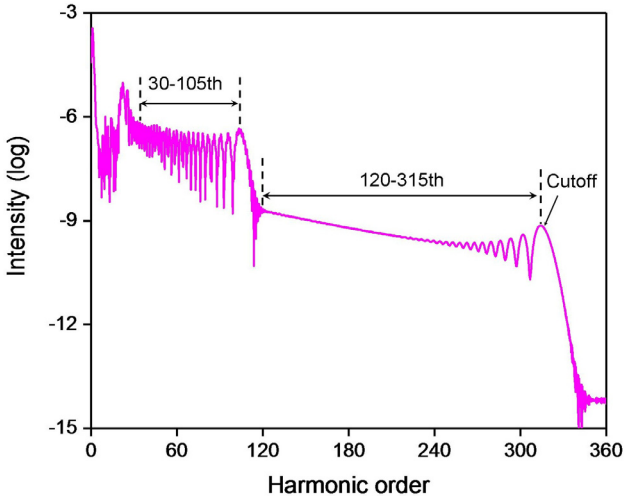

FIGURE 4. High-order harmonic spectra in log scale with two plateau regions of 30-105th and 200-250th orders.

where $E_0\,(r,z)$ and $E_1\,(r,z)$ are the BG spatial distributions with peak intensities of 0.2068a.u. and 0.16a.u., respectively. One optical cycle corresponds to the period of fundamental pulse. The envelope $f\,(t)$ is expressed as

$$f\,(t) = \exp\left[\frac{-4t^2 \ln\,(2)}{\tau^2}\right] \tag{21}$$

where $\tau = 4, 5fs$ is the full width at half maximum (FWHT) for the fundamental pulse and control pulse, respectively. According to the ionization gating mechanism, the relative phase ϕ_1 is set as zero to achieve broad supercontinuum [34].

For helium atom model, the ground state is designed as:

$$\psi(x) = Q(0.5 + \sqrt{x^2 + 0.5})\exp(-2\sqrt{x^2 + 0.5}) \tag{22}$$

with Q for the normalization coefficient. The solution range is $[-800a.u., 800a.u.]$ with Dirichlet boundary condition. The temporal and spatial spacing are designed according to stability condition with $\Delta x = 0.5a.u.$ and $\Delta t = 0.1a.u.$, respectively.

The intensity of high-order harmonic is proportional to the square of the Fourier transform mode of the electron average acceleration, which has been mentioned in Eq. (4). In Fig. 4, we plot the high-order harmonic spectra from gaseous helium irradiated by the synthesized two-color BG beam. Consistent with prediction of the ''three-step'' model, the harmonic spectra consist of three parts: the perturbative regime for low orders, the plateau for intermediate orders, and the cutoff at the highest orders. Particularly, two plateau regions of 30-105th and 120-315th orders can be observed to possess appropriate spectral intensity and exhibit regular supercontinuum characteristics, which is consistent with previous theoretical and experimental work [35], [36]. The cutoff position appears at the 315th order, which makes an agreement with the result predicted by empirical formula and experimental work, determined by:

$$E_{cutoff} = h\omega_{cutoff} \approx I_p + 3.17U_P \tag{23}$$

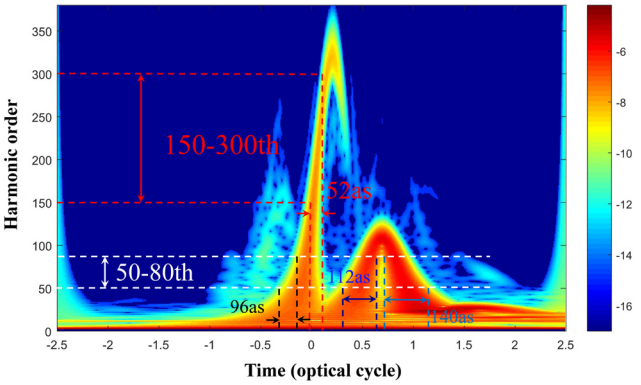

FIGURE 5. Attosecond pulses of HHG from a one dimensional helium atom model with time-frequency analysis by Morlet wavelet transform.

where I_p indicates the ionization energy and U_p indicates the ponderomotive energy [37] given by:

$$U_p = \frac{e^2 E_0^2}{4m_e\omega^2} \tag{24}$$

The quantitative comparison has demonstrated the accuracy, feasibility of the proposed method to simulate microscopic high-order harmonic generation.

Next, we carry out selective filtration of the high-order harmonic spectra. In our implementation, the window width of Morlet wavelet transform is set as $\tau = 25$. Figure 5 shows the time-frequency characteristics between radiation moment and harmonic order. The highest main peak corresponds to the second plateau region, while the adjacent main peak corresponds the first plateau region. By comparison, the highest main peak exhibits a relatively concentrated radiation range. For 50-80th orders in the first plateau region, three radiation ranges of 96as, 112as and 140as are observed due to the existence of long trajectory and short trajectory. Long trajectory is caused by earlier ionization and later recombination with electron movement for a long period, whereas short trajectory

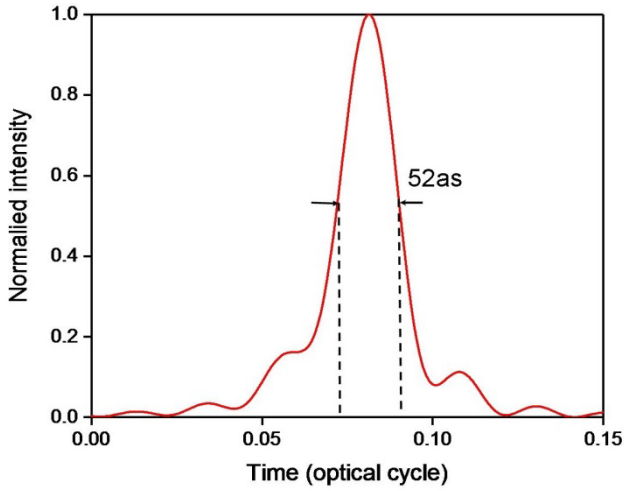

FIGURE 6. The isolated attosecond pulse of 52as synthesized by 150-300th orders harmonics.

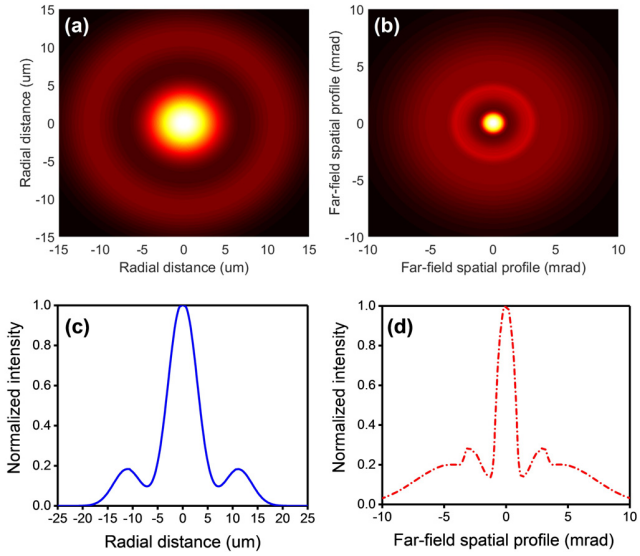

FIGURE 7. The spatial profiles of generated 52as isolated attosecond pulse with 200-250th orders harmonics. (a) and (c) correspond to radial distribution in the near field; (b) and (d) correspond to divergence angle in the far field.

is caused by later ionization and earlier recombination with electron movement for a short period. For 150-300th orders in the second plateau region, only one concentrated radiation range of 52as is observed. This is because long trajectory and short trajectory tend to coincide in the vicinity of cut-off region.

According to Eq. (7), an isolated attosecond pulse is synthesized by 150-300th orders harmonics, as shown in Fig. 6. The generated IAP performs 52as width with extremely low sides. Energy is concentrated in the main peak with 232.9∼465.9 eV board frequency band. In particular, due to the symmetry of gaseous atom, the high-order harmonic spectra have only odd orders.

Then, we concentrate on the macroscopic propagation effects of the generated 52as IAP with 150-300th orders. As illustrated in Fig. 2, a 0.5mm long gas jet is placed 2mm after the BG beam focus and the observation point in the far field is set 0.5m away from the gas jet. Only odd nonlinear polarization components are calculated and considered. With the proposed method, macroscopic propagation effects are simulated by a group of linear Maxwell's wave equations. The spatial profile of the generated IAP by two-color BG beam in helium medium is shown in Fig. 4. Figures 4(a) and 4(c) correspond to radial distribution in the near field. For observation point in the near field, the spatial profiles of generated 52as IAP present an excellent Gaussian-like with concentrated energy in the range of −7um to 7um. The far field distribution of IAP is obtained by the Hankel transform from the near field. Figures 4(b) and 4(d) correspond to divergence angle in the far field. For observation point in the far field, the divergence angle of central spot is less than 0.1° in radial direction from our calculation. The near-field and far-field results reveal that the generated 52as IAP presents a high beam quality and excellent spatial profile after macroscopic propagation in gaseous helium. In the aspects of computation, our proposed method can solve harmonic analysis of arbitrary order with only change on nonlinear polarization source, providing a promising potential on optimization design of isolated attosecond pulse.

The generated IAP are considered to have practical applications owing to the two significant advantages: (1) concentrated spot of Gaussian-like with tiny divergence angle in time domain; (2) broad supercontinuum with high photon energy range in frequency domain. In applied physics field, IAP has been widely used for dynamical probe of electronic structure and atoms on attosecond time scale [38], [39]. However, there are few applications reported in other fields. Here, our simulations reveal that IAP is extremely close to the ideal impulse in time domain. In time domain, the IAP can reflect impulse response at attosecond scale, which is an excellent input source for high power microwave protection, such as ultra-wideband GaN monolithic microwave integrated circuit (MMIC) chip [7] and beam steering antenna [8]. In recent years, quantum radar has become a hot topic, since it offers the prospect of detecting, identifying, and resolving radio frequency (RF) stealth platforms and weapons systems [9]. The IAP contains large amounts of broadband with mostly equal intensity, which can release enough high-energy photons in a very short time. In the electronic battlefield, quantum radar can make full use of IAP as transmitting signal to image the target [40]–[42].

IV. CONCLUSION

In this paper, a coherent method combined time-dependent Schrödinger equation with Maxwell's wave equation is proposed for harmonic analysis in gaseous helium. The entire simulation contains three segments: (1) microscopic harmonic generation, (2) selective filtration, (3) macroscopic propagation. We numerically investigate the high-order harmonic generation by intense driving field in gaseous helium. With time-frequency analysis by Morlet wavelet transform, specific orders are selected to synthesize an isolated

attosecond pulse. The IAP presents a high beam quality and an excellent spatial profile with Gaussian-like distribution, providing a promising potential on high power defense, quantum radar and communication. Our method offers a powerful route for computational design and optimization of isolated attosecond pulse.

ACKNOWLEDGMENT

The authors appreciate the efforts and valuable comments from the editors and anonymous reviewers.

REFERENCES

[1] E. M. Stein, *Harmonic Analysis: Real-Variable Methods, Orthogonality, and Oscillatory Integrals*. Princeton, NJ, USA: Princeton Univ. Press, 2006.
[2] W. Li, P. Li, J. Zhou, and Q. H. Liu, "Control of higher order harmonics and spurious modes for microstrip patch antennas," *IEEE Access*, vol. 6, pp. 34158–34165, 2018.
[3] Y. Grynko, T. Zentgraf, J. Förstner, and T. Meier, "Simulations of high harmonic generation from plasmonic nanoparticles in the terahertz region," *Appl. Phys. B*, vol. 122, no. 9, Sep. 2016.
[4] L. Zhang, S. Tao, Z. Fan, and R. Chen, "Efficient method for evaluation of second-harmonic generation by surface integral equation," *Opt. Express*, vol. 25, no. 23, pp. 28010–28021, 2017.
[5] J. Zhou, J. Peatross, H. C. Kapteyn, I. P. Christov, and M. M. Murnane, "Enhanced high-harmonic generation using 25 fs laser pulses," *Phys. Rev. Lett.*, vol. 76, no. 5, pp. 752–755, Jan. 1996.
[6] F. Krausz and M. Ivanov, "Attosecond physics," *Rev. Mod. Phys.*, vol. 81, no. 1, pp. 163–234, Jan./Mar. 2009.
[7] U. Schmid, H. Sledzik, P. Schuh, J. Schroth, M. Oppermann, P. Brückner, F. van Raay, R. Quay, and M. Seelmann-Eggebert, "Ultra-wideband GaN MMIC chip set and high power amplifier module for multi-function defense AESA applications," *IEEE Trans. Microw. Theory Techn.*, vol. 61, no. 8, pp. 3043–3051, Aug. 2013.
[8] Y. M. Yang, C. W. Yuan, and B. L. Qian, "Beam steering antenna for high power microwave application," *High Power Laser Particle Beams*, vol. 25, no. 10, pp. 2648–2652, 2013.
[9] M. Lanzagorta, *Quantum Radar*. San Rafael, CA, USA: Morgan & Claypool, 2011.
[10] F. Fabre, G. Petite, P. Agostini, and M. Clement, "Multiphoton above-threshold ionisation of xenon at 0.53 and 1.06 μm," *J. Phys. B*, vol. 15, no. 9, pp. 1353–1369, May 1982.
[11] P. B. Corkum, "Plasma perspective on strong field multiphoton ionization," *Phys. Rev. Lett.*, vol. 71, no. 13, pp. 1994–1997, Sep. 1993.
[12] X. Y. Z. Xiong, L. J. Jiang, Y. H. Lo, W. C. Chew, and W. E. I. Sha, "Sum-frequency and second-harmonic generation from plasmonic nonlinear nanoantennas," *Ursi Radio Sci. Bull.*, vol. 2017, no. 360, pp. 43–49, Mar. 2017.
[13] I. Ahmed, E. H. Khoo, E. Li, and R. Mittra, "A hybrid approach for solving coupled maxwell and schrödinger equations arising in the simulation of nano-devices," *IEEE Antennas Wireless Propag. Lett.*, vol. 9, pp. 914–917, 2010.
[14] M. Lewenstein, P. Balcou, A. L'Huillier, P. B. Corkum, and M. Y. Ivanov, "Theory of high-harmonic generation by low-frequency laser fields," *Phys. Rev. A, Gen. Phys.*, vol. 49, no. 3, pp. 2117–2132, Mar. 1994.
[15] M. Fang, Z. Huang, T. Koschny, and C. M. Soukoulis, "Electrodynamic modeling of quantum dot luminescence in plasmonic metamaterials," *ACS Photon.*, vol. 3, no. 4, pp. 558–563, 2016.
[16] L. Zhang, H. Zeng, and R.-S. Chen, "Full-quantum numerical scheme of finite difference time domain method for high-order harmonic generation," *IEEE J. Multiscale Multiphys. Comput. Tech.*, vol. 3, pp. 74–79, 2018.
[17] D. H. Bailey and P. N. Swarztrauber, "A fast method for the numerical evaluation of continuous Fourier and Laplace transforms," *SIAM J. Sci. Comput.*, vol. 15, no. 5, pp. 1105–1110, Sep. 1994.
[18] M. Stéphane, *A Wavelet Tour of Signal Processing*. Beijing, China: China Machine Press, 2010.
[19] X. Y. Z. Xiong, L. J. Jiang, W. E. I. Sha, Y. H. Lo, and W. C. Chew, "Compact nonlinear Yagi-Uda nanoantennas," *Sci. Rep.*, vol. 6, Jan. 2016, Art. no. 18872.
[20] M. Fang, Z. Huang, X. Y. Z. Xiong, X. Wu, and W. E. I. Sha, "Full hydrodynamic model of nonlinear electromagnetic response in metallic metamaterials," *Prog. Electromagn. Res.*, vol. 157, pp. 63–78, Oct. 2016.
[21] C. Jin, K.-H. Hong, and C. D. Lin, "Macroscopic scaling of high-order harmonics generated by two-color optimized waveforms in a hollow waveguide," *Phys. Rev. A, Gen. Phys.*, vol. 96, no. 1, Jul. 2017, Art. no. 013422.
[22] T. Morishita, A.-T. Le, Z. Chen, and C. D. Lin, "Accurate retrieval of structural information from laser-induced photoelectron and high-order harmonic spectra by few-cycle laser pulses," *Phys. Rev. Lett.*, vol. 100, no. 1, Jan. 2008, Art. no. 013903.
[23] T. Auguste, O. Gobert, and B. Carré, "Numerical study on high-order harmonic generation by a Bessel-Gauss laser beam," *Phys. Rev. A, Gen. Phys.*, vol. 78, no. 3, Sep. 2008, Art. no. 033411.
[24] L. Van Dao, K. B. Dinh, and P. Hannaford, "Generation of extreme ultraviolet radiation with a Bessel–Gaussian beam," *Appl. Phys. Lett.*, vol. 95, no. 13, 2009, Art. no. 131114.
[25] E. Schrödinger, "An undulatory theory of the mechanics of atoms and molecules," *Phys. Rev.*, vol. 28, no. 6, pp. 1049–1070, Dec. 1926.
[26] J. Crank and P. Nicolson, "A practical method for numerical evaluation of solutions of partial differential equations of the heat-conduction type," *Adv. Comput. Math.*, vol. 6, no. 1, pp. 207–226, 1996.
[27] B. C. Hall, *Quantum Theory for Mathematicians*. New York, NY, USA: Springer, 2013.
[28] T. Brabec and F. Krausz, "Nonlinear optical pulse propagation in the single-cycle regime," *Phys. Rev. Lett*, vol. 78, no. 17, pp. 3282–3285, Apr. 1997.
[29] A. E. Taylor, "L'Hospital's rule," *Amer. Math. Monthly*, vol. 59, no. 1, pp. 20–24, 1952.
[30] L. H. Thomas, "Elliptic problems in linear difference equations over a network," Watson Sci. Comput. Lab. Rept., Columbia Univ., New York, NY, USA, Tech. Rep., 1949.
[31] M. V. Ammosov, N. B. Delone, A. Perelomov, V. Popov, M. Terent'ev, G. L. Yudin, M. Y. Ivanov, and V. Krainov, "Tunnel ionization of complex atoms and of atomic ions in an alternating electric field," *Sov. Phys.-JETP*, vol. 64, no. 1191, p. 26, 1986.
[32] X. Wang, J. Tian, and J. H. Eberly, "Extended virtual detector theory for strong-field atomic ionization," *Phys. Rev. Lett.*, vol. 110, no. 24, Jun. 2013, Art. no. 243001.
[33] Q. Su and J. H. Eberly, "Model atom for multiphoton physics," *Phys. Rev. A, Gen. Phys.*, vol. 44, no. 9, pp. 5997–6008, Nov. 1991.
[34] P. Lan, P. Lu, W. Cao, Y. Li, and X. Wang, "Attosecond ionization gating for isolated attosecond electron wave packet and broadband attosecond XUV pulses," *Phys. Rev. A, Gen. Phys.*, vol. 76, no. 5, Nov. 2007, Art. no. 051801(R).
[35] E. Balogh, K. Kovács, K. Varjú, and V. Toşa, "A case study for terahertz-assisted single attosecond pulse generation," *J. Phys. B, At. Mol. Opt. Phys.*, vol. 45, no. 7, 2012, Art. no. 074022.
[36] E. J. Takahashi, P. Lan, O. D. Mücke, Y. Nabekawa, and K. Midorikawa, "Infrared two-color multicycle laser field synthesis for generating an intense attosecond pulse," *Phys. Rev. Lett.*, vol. 104, no. 23, Jun. 2010, Art. no. 233901.
[37] J.-P. Connerade, *Highly Excited Atoms*. Cambridge, U.K.: Cambridge Univ. Press, 1998.
[38] F. Calegari, D. Ayuso, L. Belshaw, S. De Camillis, S. Anumula, F. Frassetto, L. Poletto, A. Palacios, P. Decleva, J. B. Greenwood, F. Martín, M. Nisoli, and A. Trabattoni, "Ultrafast electron dynamics in phenylalanine initiated by attosecond pulses," *Science*, vol. 346, no. 6207, pp. 336–339, Oct. 2014.
[39] M. Chini, K. Zhao, and Z. Chang, "The generation, characterization and applications of broadband isolated attosecond pulses," *Nature Photon.*, vol. 8, no. 27, pp. 178–186, Mar. 2014.
[40] M. J. Brandsema, R. M. Narayanan, and M. Lanzagorta, "Theoretical and computational analysis of the quantum radar cross section for simple geometrical targets," *Quantum Inf. Process.*, vol. 16, no. 1, p. 32, Jan. 2017.
[41] C. H. Fang, "The simulation and analysis of quantum radar cross section for three-dimensional convex targets," *IEEE Photon. J.*, vol. 10, no. 1, Feb. 2018, Art. no. 7500308.
[42] C. H. Fang, H. Tan, and Q. F. Liu, "The calculation and analysis of the bistatic quantum radar cross section for the typical 2-D plate," *IEEE Photon. J.*, vol. 10, no. 2, Apr. 2018, Art. no. 7500614.

LEI ZHANG received the B.Sc. degree in electronic information engineering from the Nanjing University of Science and Technology (NJUST), Nanjing, China, in 2014, where he is currently pursuing the Ph.D. degree in electromagnetic fields and microwave technology with the Department of Communication Engineering.

His research interests include computational electromagnetics, quantum electromagnetics, and nonlinear second- and high-order harmonic generation.

ZHENHONG FAN was born in Jiangsu, China, in 1978. He received the M.Sc. and Ph.D. degrees in electromagnetic field and microwave technique from the Nanjing University of Science and Technology (NJUST), Nanjing, China, in 2003 and 2007, respectively.

In 2006, he was a Research Assistant with the Center of wireless Communication, City University of Hong Kong. He is currently a Professor of electronic engineering with NJUST. He is the author or a coauthor of over 50 technical articles. His current research interests include computational electromagnetics, and electromagnetic scattering and radiation.

RUSHAN CHEN (M'01–SM'15) was born in Jiangsu, China. He received the B.Sc. and M.Sc. degrees from the Department of Radio Engineering, Southeast University, China, in 1987 and 1990, respectively, and the Ph.D. degree from the Department of Electronic Engineering, City University of Hong Kong, in 2001.

He joined the Department of Electrical Engineering, Nanjing University of Science and Technology (NJUST), China, where he became a Teaching Assistant, in 1990, and a Lecturer, in 1992. Since September 1996, he has been a Visiting Scholar with the Department of Electronic Engineering, City University of Hong Kong, first as a Research Associate and then as a Senior Research Associate, in July 1997, a Research Fellow, in April 1998, and a Senior Research Fellow, in 1999. From June 1999 to September 1999, he was a Visiting Scholar with Montreal University, Canada. In September 1999, he was promoted to Full Professor and Associate Director of the Microwave and Communication Research Center, NJUST, and in 2007, he was appointed as the Head of the Department of Communication Engineering, NJUST. He was appointed as the Dean of the School of Communication and Information Engineering, Nanjing University of Posts and Telecommunications, in 2009. In 2011, he was appointed as the Vice Dean of the School of Electrical Engineering and Optical Technique, NJUST. He is currently a Principal Investigator of more than ten national projects. His research interests mainly include computational electromagnetics, microwave integrated circuit and nonlinear theory, smart antenna in communications and radar engineering, microwave material and measurement, and RF-integrated circuits. He has authored or coauthored more than 260 articles, including over 180 articles in international journals.

Prof. Chen is an Expert enjoying the special government allowance, a member of the Electronic Science and Technology Group, a Fellow of the Chinese Institute of Electronics (CIE), the Vice-President of Microwave Society of CIE and IEEE MTT/APS/EMC Nanjing Chapter, and an Associate Editor of the *International Journal of Electronics*. He was a recipient of the Foundation for China Distinguished Young Investigators presented by the China NSF, a Cheung Kong Scholar of the China Ministry of Education, and the New Century Billion Talents Award. He received several best paper awards from the National and International Conferences and Organizations. He serves as a Reviewer for many technical journals, such as the IEEE Transactions on Antennas and Propagation, IEEE Transactions on Microwave Theory and Techniques, and *Chinese Physics*.